University of Strathclyde Glasgow

This version is available at https://strathprints.strath.ac.uk/56431/

epl draft

Evidence of high-n hollow ion emission from Si ions pumped by ultraintense x-rays from relativistic laser plasma

J. Colgan[1], A. Ya. Faenov[2,3], S. A. Pikuz[3,4], E. Tubman[5], N. M. H. Butler[6], J. Abdallah, Jr.[1], R. J. Dance[6], T. A. Pikuz[3,7], I. Yu. Skobelev[3,4], M. A. Alkhimova[3,4], N. Booth[8], J. Green[8], C. Gregory[8], A. Andreev[9,10], R. Lötzsch[11], I. Uschmann[11], A. Zhidkov[7], R. Kodama[2,7], P. McKenna[6], and N. Woolsey[5]

[1] *Theoretical Division, Los Alamos National Laboratory, Los Alamos, NM 87545, USA*
[2] *Institute for Academic Initiatives, Osaka University, Suita, Osaka 565-0871, Japan,*
[3] *Joint Institute for High Temperatures, Russian Academy of Sciences, Moscow 125412, Russia*
[4] *National Research Nuclear University MEPhI, Moscow, 115409, Russia*
[5] *York Plasma Institute, Department of Physics, University of York, York YO10 5DD, United Kingdom*
[6] *SUPA, Department of Physics, University of Strathclyde, Glasgow G4 ONG, United Kingdom*
[7] *PPC Osaka University and JST, CREST, 2-1, Yamadaoka, Suita, Osaka 565-0871, Japan*
[8] *Central Laser Facility, STFC Rutherford Appleton Laboratory, Didcot, Oxfordshire OX11 0QX, United Kingdom*
[9] *Max Born Institute, Berlin 12489, Max-Born str. 2a, Berlin, Germany*
[10] *ELI-ALPS, Szeged H-6720, Hungary*
[11] *Institut für Optik und Quantenelektronic, Friedrich-Schiller-Universität Jena, Max-Wien Platz 1, D-07743 Jena, Germany*

Abstract – We report on the first observation of high-n hollow ions (ions having no electrons in the K or L shells) produced in Si targets via pumping by ultra-intense x-ray radiation produced in intense laser-plasma interactions reaching the radiation dominant kinetics regime. The existence of these new types of hollow ions in high energy density plasma has been found via observation of highly-resolved x-ray emission spectra of silicon plasma, and confirmed by plasma kinetics calculations, underscoring the ability of powerful radiation sources to fully strip electrons from the inner-most shells of light atoms. Hollow ions spectral diagnostics provide a unique opportunity to characterize powerful x-ray radiation of laboratory and astrophysical plasmas.

The ability of bright photon sources to rapidly remove the inner-shell electrons from atoms has become an exciting area of research in recent years since it encompasses a region that lies on the boundary of atomic and plasma physics. This is in part due to the increasing availability of such radiation-generating sources as XFELs [1–5] and next-generation petawatt laser facilities that can generate high-intensity x-ray fields [6]. These experimen-

tal platforms have been used to create novel states of matter with empty inner sub-shells [2–11], explore the phenomena of continuum lowering [12] and of saturable absorption [13], and to explore the regime where the radiation interaction dominates the plasma kinetics [16]. Such investigations, as well as complementary simulations (for example, [14,15]) help our understanding of high energy density plasmas of importance in astrophysics [17–19], inertial confinement fusion [20], and the bright x-ray sources are also of use in biological imaging and in materials science [21]. Recent reviews [10,11,22] have explored in detail the mechanisms of hollow ion emission in a variety of experimental contexts.

The term 'hollow ion' has had a number of definitions over the years [23, 24] but is generally taken to mean atomic states in which the K shell (and sometimes L shell) is partly or fully stripped. Recent petawatt laser measurements on thin Al targets [7] indicated the formation of ions with empty K-shells, identified by x-ray emission from the transition of a $2p$ electron into the $1s$ subshell. Indeed, all reported observations of hollow ions have used the same $2p \rightarrow 1s$ transition to identify such states (whether single- or double-core hole states). One generally requires a strong driving mechanism to populate the hollow ion states. A strong radiation field [8] has been shown to be much more efficient at ionizing the K-shell compared to, say, collisions with hot electrons.

In this Letter, we demonstrate for the first time that hollow ions can be identified that have no electrons in both the K or L shells, labeling such states 'high-n hollow ions'. Such states in Si are identified by the emission of photons corresponding to the $3p \rightarrow 1s$ transition that occurs in a lower wavelength range, between the Ly$_\beta$ and He$_\beta$ line positions, compared to the previously-observed hollow ion emission that occurs between the Ly$_\alpha$ and He$_\alpha$ line positions. A diagram of observed transitions in Si that are discussed in this paper is presented in Fig. 1. The hollow ion emission characterized by $2p \rightarrow 1s$ transitions in moderately ionized ions occurs around 6.4 Å (for double-core hole states) and around 6.9 Å (for single-core hole states). high-n hollow ion emission occurs around 5.4 Å, i.e. between the Ly$_\beta$ (at 5.2 Å) and He$_\beta$ (at 5.68 Å) line positions. Observation of such emission is made possible by high-resolution x-ray spectrometers (positioned around the experiment) that cover an extended wavelength range, as shown in Fig. 2a.

A schematic of the experimental set-up and a diagram of hollow ion formation and detection in our experiments are shown in Fig. 2. The measurements were made at the Vulcan Petawatt (PW) laser facility at the Rutherford Appleton Laboratory [25], which generates a beam using OPCPA technology with a central wavelength of 1054 nm and FWHM duration $\sim$ 0.5–1 ps. In this experiment approximately 114 J was delivered to the target surface by a p-polarized laser pulse, focused by an f/3 off-axis parabola at an incident angle of 45° from its surface normal. The energy was contained in a focal spot with diameter of 7 μm, resulting in an intensity of 3×10^{20} W/cm^2 on the target, which comprised 2 μm Si wafers, sandwiched between two 1.6 μm CH layers. **The contrast of the laser was 10^{-10}, and such a high contrast was important in identifying and interpreting the hollow atom emission.** Four Focusing Spectrometers with Spatial Resolution (FSSR) [26] captured the resultant emission, with two positioned in front of the target and two behind, with two wavelength ranges covered as indicated in Fig. 3. The Front 1 and Rear 1 spectrometers used mica spherically bent crystals with R=150 and R=100 mm radius of curvature, respectively, enabling spectral measurements in the third order of mica crystal reflection at 4.7–5.6 Å. The Front 2 and Rear 2 spectrometers were equipped with quartz (10-10, 2nd 8.5 Å) spherically bent crystals with R=150 and R=100 mm radius of curvature, respectively, enabling measurements to be made in the spectral range 6.0–7.2 Å. Image plate detectors covered by different filters were used for the diagnosis of spectra from all spectrometers, with the exception of the Front 1 spectrometer in which a back-illuminated CCD was used. Strong magnets were placed in front of the spectrometers in order to reduce background x-ray noise generated by fast electrons. The spectrometers were cross-calibrated so that the intensity from all spectrometers are comparable.

We observe experimentally that the emission recorded on the front spectrometers is in
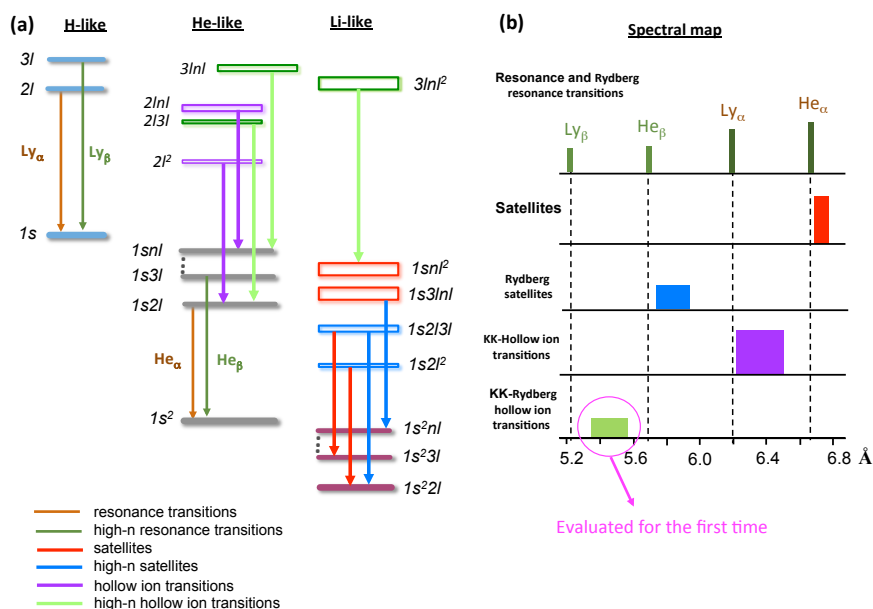
Fig. 1: Schematic diagram of the hollow ion and high-n hollow ion line positions in H-like through Li-like Si ions: (a) the type of transition; (b) the wavelength positions. The resonance and satellite transitions have one electron in the K-shell in the upper levels, whereas hollow ion and high-n hollow ion transitions have no K-shell electrons in the upper levels. Furthermore, the high-n hollow ions have no electrons in the L-shell in the upper levels.

general more intense than that of the rear spectrometers. However, we find that the ratio of the Ly_α to He_α lines (at 6.18 Å and 6.65 Å respectively) is larger from the Rear 2 spectrometer than from the Front 2 spectrometer. At first this seems to imply that the bulk plasma temperature is hotter on the rear surface than on the front surface, which is at odds with the lower intensity recorded on the rear spectrometers compared to the front. However, we find that emission is also observed between the Ly_α and He_α lines. Such emission arises from KK hollow ion transitions [7] and implies that hollow ion emission is contributing strongly to the spectrum measured by the Rear 2 spectrometer. We have performed plasma kinetics modeling calculations for Si using the Los Alamos suite of atomic physics codes (for an overview, see [27]) to help understand these measurements. Atomic structure and collision calculations were performed [28–30] and the ATOMIC code [31–33] was used to produce emission spectra for a variety of plasma temperatures and densities.

The modeling of the complex emission spectra measured from this plasma is difficult due to the spatially and temporally integrated nature of the recorded spectra. In principle, hydrodynamic simulations could be used to predict the
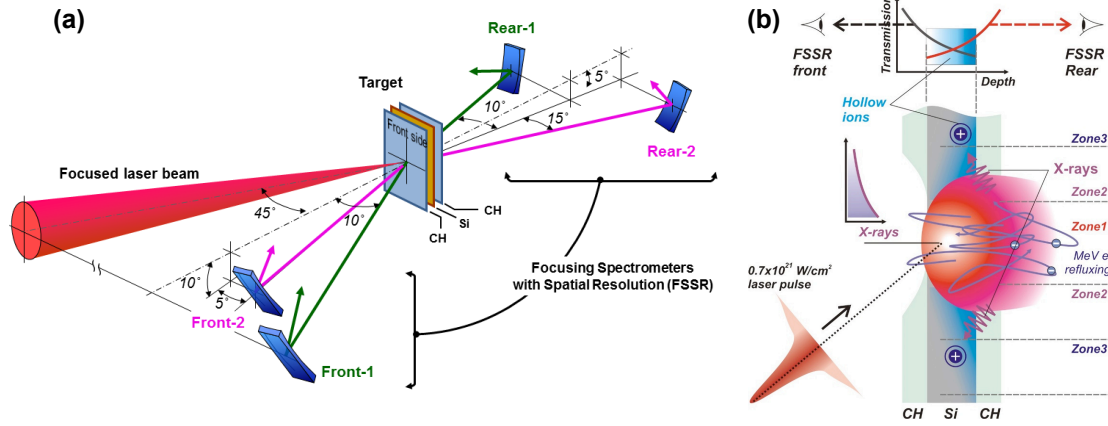
Fig. 2: (a) Experimental design. (b): A schematic diagram of hollow ion formation by the ultraintense optical laser pulse and its detection from both sides of the target. A laser field in the central area of the focal spot of the target accelerates multi-MeV electrons along the laser beam propagation. Refluxing electrons generate bright x-ray radiation with photons of ∼keV energies, which creates hollow ions in the outer area of the focal spot. X-ray spectra of hollow ions, emitted by the plasma periphery and measured by FSSR spectrometers from the front and rear sides of target, have different intensities due to differences in absorption of x-ray radiation, which reach the front and rear sides spectrometers. The stronger x-ray pump intensity of the rear side compared with the front side target surfaces is due to target bending from laser radiation pressure from the relativistic laser beam.

108 density and temperature profile of the plasma as a function of space and time -
109 however such simulations are quite difficult to perform and also require various
110 assumptions concerning laser energy absorption, material properties, etc. How-
111 ever, we have found from experience that the complex emission spectra can be
112 reasonably modeled by ATOMIC calculations that assume that the plasma is
113 (arbitrarily) divided into just a few zones at particular temperatures and den-
114 sities. This allows some insight into the conditions that may exist within the
115 plasma, as well as allowing an understanding of what emission features arise
116 from plasma at a particular set of conditions.
117   In this case, we find that the measured emission spectra can be reasonably

reproduced by 3 plasma zones, as indicated in fig. 2b. The first, central, zone contains bulk plasma at high electron temperatures (kT_e) of 400 eV (for the rear side of the target) or 550 eV (front side) and an electron density (N_e) of 10^{22} cm^{-3}. This is the region that has directly absorbed most of the laser energy, and as a result, the target is highly ionized.

The second plasma zone surrounds the central zone and is postulated to be at a lower electron temperature of 180 eV and an N_e of 3×10^{23} cm^{-3} (close to solid density conditions). This zone feels a radiation field at a temperature of 2 keV, which arises from the radiation (mostly Bremsstrahlung) emitted from the high energy refluxing electrons formed in the focus of the laser spot. The third plasma zone lies beyond the second plasma zone, and is thought to be at a cooler temperature of 10 eV, again with an N_e of 3×10^{23} cm^{-3}. This zone feels a radiation field at 3 keV. We also postulate that a portion of this zone may also see an enhanced (by a factor of 5) radiation field, the reason for which is discussed in detail in the following paragraphs. All our ATOMIC calculations include continuum lowering [34], a 1% hot electron component, and self-absorption effects via escape factors assuming a 6μm thickness. The theoretical modeling calculations show that, while a bulk plasma at **zone 1** conditions provides a reasonable match to the Ly$_\alpha$ and He$_\alpha$ lines (as well as their satellites), we require additional emission from the other plasma zones (see fig. 2b) to match the observed spectrum. Because of the time-integrated nature of the measured spectrum we had to make assumptions about the duration time of the emission from the zones. Generally, the emission from zones 2 and 3 was assumed to be of much shorter duration than the emission from zone 1. An ATOMIC calculation at zone 2 conditions produces significant emission around 6.2 Å, enhancing the emission at exactly the Ly$_\alpha$ wavelength. Addition of another ATOMIC calculation at similar conditions but with a smaller kT_e of 90 eV also improves the comparison with the measured spectrum. Thus, without consideration of emission from hollow ions, **that are only prominent when a strong radiation field is included in the modeling,** one would estimate a hotter temperature in this plasma than may actually exist.

Further evidence for the existence of hollow ion emission is found from ATOMIC calculations at **zone 3 conditions** which provides neutral K-shell emission lines around 7.1 Å (as well as weaker lines around 6.5 Å). If we postulate that the radiation field produced by the refluxing electrons may be enhanced in some spatial regions (by a factor of 5 in this case), as discussed in detail recently [16], we find that such ATOMIC calculations predict weak emission around 6.4 Å, in good agreement with the measured spectrum. This indicates that the plasma conditions under investigation may be entering the radiation-dominated kinetic regime (RDKR) as also found in ultra-intense laser measurements performed recently [7–9, 16].

Returning to the spectrum recorded on the Front 2 spectrometer (Fig. 3b), we find that it is quite well matched by an ATOMIC calculation at zone 1 conditions of kT_e of 550 eV and N_e of 10^{22} cm^{-3}, and that the contributions from plasma zones 2 and 3 under the influence of the x-ray field are much smaller. This suggests that hollow ion emission is only observed (in the longer wavelength region) from the rear of the target as shown in Fig. 3d. We also note that the He$_\alpha$ line and its satellite features are shifted in the measurement compared to the calculation by about 0.02 Å. This is due to fast ion motion of the He-like ions, which corresponds to a ion motion speed of approximately 10^8 cm/s with ion energy of ∼150 keV. Such an effect has previously been observed [35].

The spectra recorded by the Front 1 and Rear 1 spectrometers (left panels of Fig. 3) cover the wavelength range of Si that includes emission from the Ly$_\beta$ (5.22 Å), Ly$_\gamma$ (4.95 Å), and He$_\gamma$ (5.41 Å) lines. While these lines are reasonably prominent in the measured data, we also find significant emission between these lines. ATOMIC calculations from bulk plasma at nominal conditions of electron temperature (kT_e) of 400 eV (rear spectrometer) or 550 eV (front spectrometer) and electron density (N_e) of 10^{22} cm^{-3} provide a good match to the

He-like and H-like features, but do not produce emission in the regions between these lines. However, ATOMIC calculations at lower electron temperatures (90 eV), which were also used to explain the hollow ion spectra formation from the Front 2 and Rear 2 spectrometers, and that include a x-ray radiation field (at 2 keV), *do* provide such emission and also improve the agreement with the measured emission around 5.0 Å. The transitions that are prominent from such calculations arise from what we term *high-n hollow ions*, that is, transitions from the $3p$ subshell to the empty $1s$ (K) shell of Li-like (and other) Si ions. We are unaware of any previous observations of such transitions, although a previous study [36] postulated the existence of such transitions in quasi-continuous spectra. **These high-n hollow ions lie near the Ly$_\beta$ lines and are of similar intensity. Thus, it is important to consider such states when analyzing the role of ionization potential lowering in dense plasmas.** We also remark that calculations at lower temperatures (eg 10 eV) produce no transitions in this wavelength region even with an intense x-ray field.

To further illustrate the important role played by the x-ray radiation, in Figs. 4 and 5 we present ATOMIC calculations at various electron temperatures made without the radiation field for various fractions of hot electrons (at a temperature of 10 keV). We find that even somewhat large hot electron fractions of 10% or more (see Fig. 5) do not produce KK transitions, especially in the region around 6.4 Å, and between 5.2 and 5.4 Å. We also note that the intensity of emission from the ATOMIC calculations with only hot electrons is one or more orders of magnitude smaller than the emission found when a x-ray radiation field is used in the calculations. Such calculations support our assertion that an intense x-ray radiation field, produced by the refluxing electrons through the thin target, is the most plausible mechanism for production of the KK hollow ion and high-n hollow ion emission that is found experimentally.

The finding that hollow ion emission is mostly observed from the rear side of the target provides further confidence that the hollow ions are driven by ultra-intense x-ray radiation emission by plasma approaching the RDKR. Indeed, the x-ray pumping source was found to be situated behind the primary, laser-facing, CH foil, curved inward during interaction with the incident laser pulse (and pre-pulse). The absorption of this radiation becomes important due to its role in producing the radiation field. The experimentally observed Doppler shifts of spectral lines confirm the movement of the critical surface toward the x-ray source. The mean free path of x-rays can be easily estimated using the Kramers approximation for photoionization cross-section as $l^{-1} = 8 \times 10^{-18} N_Z (I_z/\hbar\omega)^3/Z^2$ cm^{-1} where I_Z is the ionization potential, N_Z the ion density, Z the ion charge, and $\hbar\omega$ the x-ray energy. Assuming $\hbar\omega \approx I_Z$ one finds that for solid density and $Z = 10$ that $l \approx 2.5\ \mu$m. That means in a curved target, x-rays interact mainly with the rear surface. This also explains the difference in plasma temperatures seen from the front and rear sides of the target.

It should also be noted that even simple detection of hollow ion spectra allows an estimation of the intensity of x-rays pumping the plasma. The hollow ions are excited from autoionizing ionic states by photoionization. To produce a sufficient number of hollow ions the photoionization must be the main channel of the autoionizing state decay. It means that condition $(I_X/\hbar\omega)\sigma^{ph} \geq G$ must be satisfied (where I_X is the x-ray pumping flux, $\hbar\omega$ is the energy of the x-ray photon, σ^{ph} is the photoionization cross section and G is the probability of autoionization). An estimate finds that for the Si XIII ion the x-ray radiation will produce a sufficient number of hollow ions when I_X is about 10^{18} W/cm^2 or higher. The comparison of the experimental spectra with theoretical spectra allows one to determine x-ray intensity more exactly.

An alternative estimation of the x-ray flux I_X can also be made by considering a beam of fast electrons with the number $N_{eh} \approx [0.03 + \eta I_{18}/(30 + I_{18})]\epsilon_L/\epsilon_{eh}$, (where η is the absorption coefficient, ϵ_L is the laser energy and I$_{18}$ is the laser intensity in units of 10^{18} W/cm^2) and with energy ϵ_{eh}. The power generated by a single electron can be estimated [38] (using a classical approach [37]) as $W \approx e^2 c \beta^4 \gamma^4/d^2$, where $\beta = v/c$, γ is the electron relativistic factor, and d is the electron trajectory radius. Since an electron radiates in the
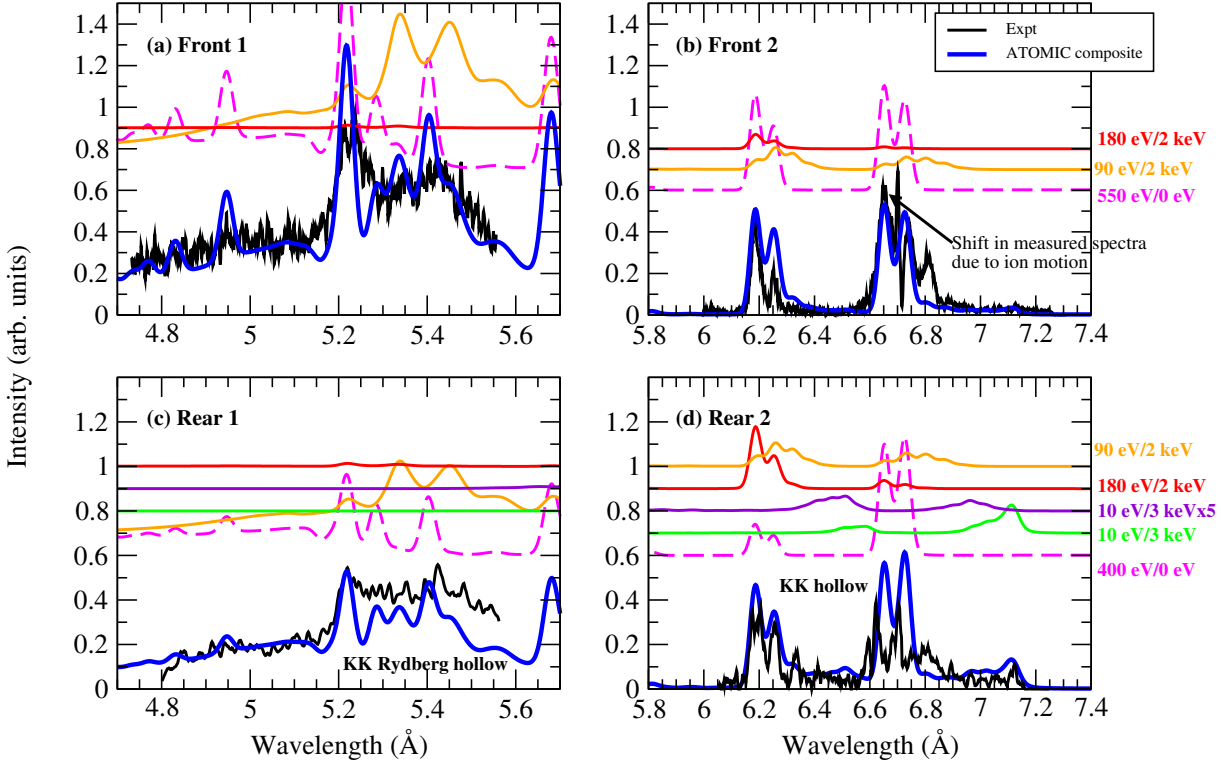
Fig. 3: Comparison of measured spectra from the four spectrometers shown in Fig. 2 and composite ATOMIC calculations as indicated, assuming emission from various plasma zones (see fig. 2b). The experimental spectra are presented with a common calibration so that the intensities in each panel are comparable. The thick blue lines represent the composite ATOMIC calculations that are the sum of calculations at specific temperatures and densities as follows. The ATOMIC calculations are performed for a bulk electron temperature (kT_e) of 550 eV for the front spectrometers and a kT_e of 400 eV for the rear spectrometers, for an electron density (N_e) of 10^{22} cm^{-3} (for zone 1). We include contributions from calculations at kT_e= 180 eV and kT_e=90 eV, both using a radiation field (kT_r) of 2 keV and N_e=3 × 10^{23} cm^{-3} (for zone 2). The comparisons of the spectra from the rear spectrometers also include a calculation at kT_e=10 eV, kT_r=3 keV, as well as a calculation at kT_e=10 eV, with a kT_r=3 keV that is enhanced by a factor of 5 (all at N_e=3 × 10^{23} cm^{-3}) (for zone 3). All calculations include a 1% hot electron component at a temperature of 10 keV, continuum lowering effects [34], and self-absorption effects assuming a 6 μm thickness. The individual ATOMIC calculations are offset for clarity. The proportion of radiation from each plasma zone is adjusted to match the measured spectra, and implies that the radiation from the bulk plasma (at a high electron temperature and N_e=10^{22} cm^{-3}) lasts much longer than the radiation from the other plasma regions.
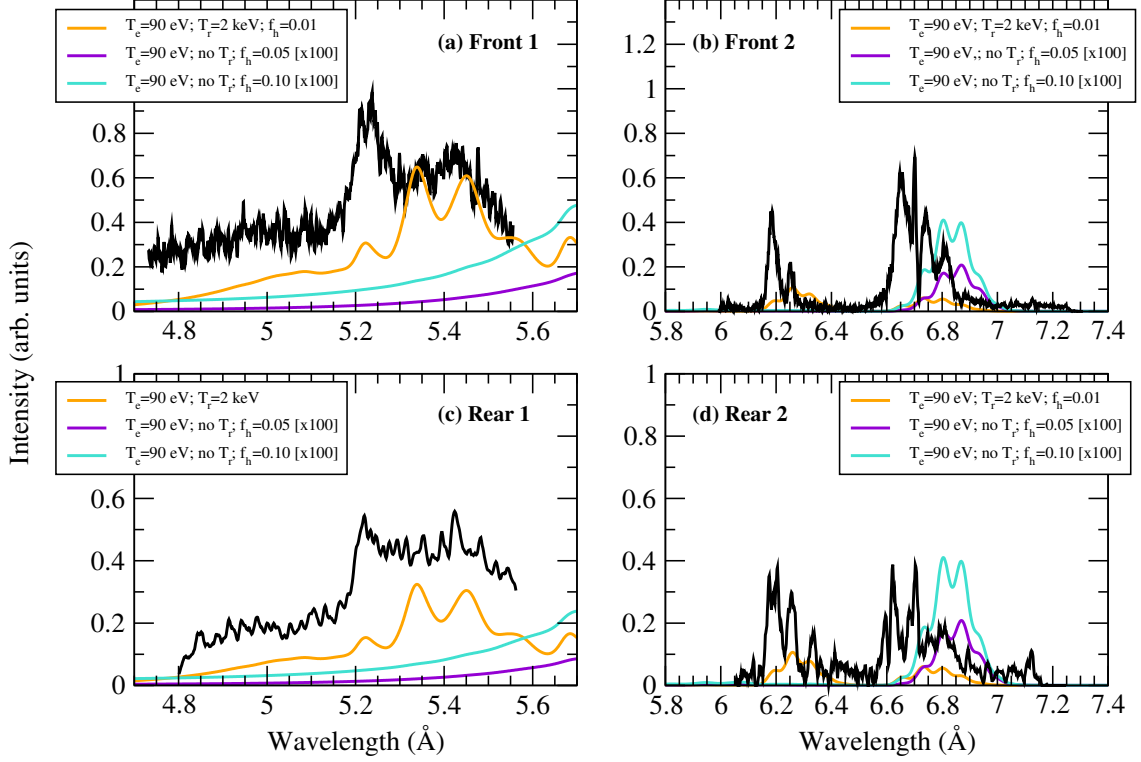
Fig. 4: Comparisons of the measured spectra and ATOMIC calculations at kT_e=90 eV (all at N_e=3 × 10^{23} cm^{-3}). The orange lines show calculations using kT_r=2 keV and 1% hot electrons. The purple and blue lines show calculations using no radiation field, but with 5% and 10% hot electron fraction respectively. Note that the latter two calculations are multiplied by 100 for better visual comparison.

frequency range close to $\omega_0\gamma^3$, one can estimate the x-ray flux with the number of electron refluxing through the target (N_{rec}) as $\frac{e^2c}{d^2}(\frac{\omega}{\omega_0})^{4/3}N_{rec}N_{eh}/D_L^2$, with D_L the laser spot size. For a thin foil, $d \sim 2$ μm, $D_L \sim 10$ μm, and for X-rays of energy $\omega \sim 5$ keV, laser frequency $\omega_0 \sim 1$ eV, $N_{rec} \approx 1$, and $I_L = 3 \times 10^{20}$ W/cm^2 the x-ray flux is then approximately 1×10^{18} W/cm^2.

Our calculations show that observable features of the hollow ion spectra are sensitive to such plasma parameters as density, temperature, hot electron fraction, and intensity of the short-wavelength pumping radiation (see figs. 3-5). The last dependence is the most important for plasma diagnostic applications. In the last few decades a number of diagnostics have been developed for analysis of high-temperature plasma. Such diagnostics allow the measurement of important plasma parameters such as plasma density, plasma temperature, and hot electron fraction. However, no methods exist for determination of the ultraintense x-ray radiation that can strongly perturb the plasma. It seems feasible that observation of high-n hollow ion transitions may now be used for this purpose. This possibility has
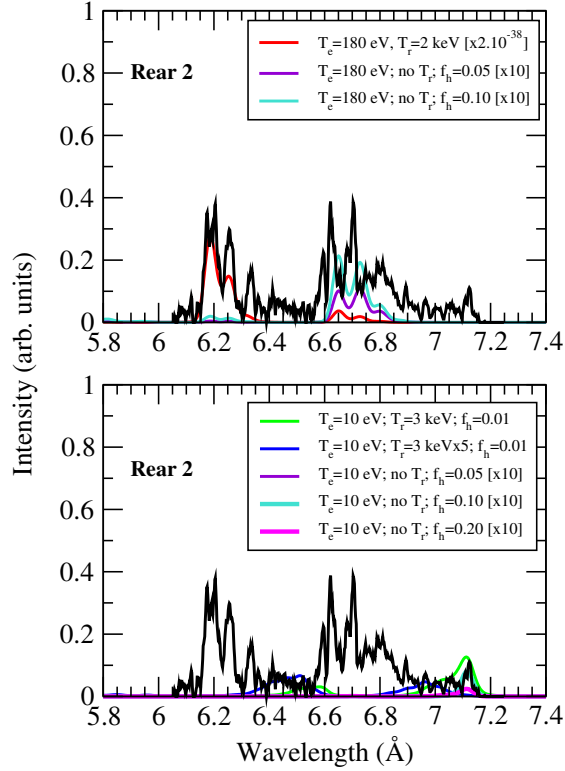
Fig. 5: Comparisons of the measured spectra from the Rear 2 spectrometer with ATOMIC calculations (all at $N_e = 3 \times 10^{23}$ cm^{-3}). The upper panel shows calculations at $kT_e = 180$ eV with a radiation field of 2 keV (red line); no radiation field at 5% hot electrons (purple line), and no radiation field and 10% hot electrons (blue line). The lower panel shows a similar comparison except for Te=10 eV. We also show a further calculation with no radiation field and with 20% hot electrons (pink line).

* * *

implications for the diagnostics of near-solid-density laboratory and astrophysical plasmas pumped by intense x-rays and/or electron beams.

REFERENCES

[1] YOUNG L. *et al.*, *Nature*, **466** (2010) 56.
[2] VINKO S. M. *et al.*, *Nature*, **482** (2012) 59.
[3] NAGLER B. *et al.*, *Nature Phys.*, **5** (2009) 693.
[4] WALDROP M. M., *Nature*, **505** (2014) 604.
[5] MIMURA H. *et al.*, *Nature Comm.*, **5** (2014) 3539.
[6] PIKUZ S. A. *et al.*, *Physics-Uspekhi*, **57** (2014) 702.
[7] COLGAN J. *et al.*, *Phys. Rev. Letts.*, **110** (2013) 125001.
[8] PIKUZ S. A. *et al.*, *High Energy Density Phys.*, **9** (2013) 560.
[9] HANSEN S. B. *et al.*, *Phys. of Plasmas*, **21** (2014) 031213.
[10] SKOBELEV I. YU. *et al.*, *Physics-Uspekhi*, **55** (2012) 47.
[11] FAENOV A. YA. *et al.*, *Laser Part. Beams*, **33** (2015) 27–39.
[12] CIRICOSTA O. *et al.*, *Phys. Rev. Letts.*, **109** (2012) 065002.
[13] RACKSTRAW D. S. *et al.*, *Phys. Rev. Letts.*, **114** (2015) 015003.
[14] ROSMEJ F. B., *Europhys. Lett.*, **55** (2001) 472.
[15] ROSMEJ F. B. and LEE R. W., *Europhys. Lett.*, **77** (2007) 24001.
[16] FAENOV A. YA. *et al.*, *Sci. Reports*, **5** (2015) 13436.
[17] BEIERSDORFER P. *et al.*, *Ann. Review Astron. & Astrophys.*, **41** (2003) 343.
[18] BEHAR E., SAKO M. and KAHN S. M., *Ap. J.*, **563** (2001) 497.
[19] SAVIN D. W. *et al.*, *Rep. Prog. Phys.*, **75** (2012) 036901.
[20] ATZENI S. and MEYER-TER-VEHN J., *The Physics of Inertial Fusion* (Clarendon Press, Oxford) 2004.
[21] BRENNER C. M. *et al.*, *Plasma Phys. Contr. Fusion*, **58** (2016) 014039.
[22] ROSMEJ F. B. *et al.*, *J. Phys. B*, **48** (2015) 224005
[23] BRIAND J.-P. *et al.*, *Phys. Rev. Letts.*, **65** (1990) 159.
[24] MCPHERSON A. *et al.*, *Nature*, **370** (1994) 631.
[25] DANSON C. N. *et al.*, *Laser and Particle Beams*, **23** (2005) 87.
[26] FAENOV A. YA. *et al.*, *Physica Scripta*, **50** (1994) 333.
[27] FONTES C. J. *et al.*, *J. Phys. B*, **48** (2015) 144014.
[28] COWAN R. D., *The Theory of Atomic Structure and Spectra* (University of California Press, Berkeley) 1981.
[29] ABDALLAH J., CLARK R. E. H. and COWAN R. D., *Los Alamos National Laboratory, Los Alamos Manual No. LA 11436-M-I*, **1988** (.)
[30] CLARK R. E. H., ABDALLAH JR J. and MANN J. B., *Ap. J.*, **381** (1991) 597.
[31] MAGEE N. H. *et al.*, *14th Topical Conference on Atomic Processes in Plasmas*, edited by J.S. COHEN, S. MAZEVET, AND D. P. KILCREASE (AIP Conference Proceedings, New York) 2004, p. 168–179.
[32] HAKEL P. *et al.*, *J. Quant. Spectr. Rad. Transfer*, **99** (2006) 265.
[33] MAZEVET S. and ABDALLAH, JR. J., *J. Phys. B*, **39** (2006) 3419.
[34] STEWART J. C. and PYATT, JR. K. D., *Ap. J.*, **144** (1966) 1203.
[35] BELYAEV V. S. *et al.*, *JETP Letters*, **81** (2005) 616.
[36] FAENOV A. *et al.*, *Physica Scripta*, **T80** (1999) 536.
[37] ANDREEV A. A. and PLATONOV K. YU., *Laser and Particle Beams*, **18** (2000) 81.
[38] TERNOV M., *Physics-Uspekhi*, **38** (1995) 409.